J. Water Environ. Nanotechnol., 5(3): 256-269 Summer 2020

ORIGINAL RESEARCH PAPER

Basic Dyes Removal by Adsorption Process Using Magnetic Fucus Vesiculosus (Brown Algae)

Hessam Jafari[1], Gholam Reza Mahdavinia[1*], Bagher Kazemi Heragh[2], Shahrzad Javanshir[2], Samira Alinavaz[1]

[1] Polymer Research Laboratory, Department of Chemistry, Faculty of Science, University of Maragheh, 55181-83111, Maragheh, Iran.
[2] Department of Chemistry, Iran University of Science and Technology, Tehran 16846-13114, Iran.

Received: 2020-05-18 Accepted: 2020-07-16 Published: 2020-08-01

ABSTRACT

In this project, new magnetic *Fucus vesiculosus* (m-FV) nanoparticles with a high adsorption capacity of cationic dyes were prepared. To reach a nanocomposite with effective performance, *Fucus vesiculosus* (FV) was modified using ultrasound. Then, the Fe^{2+}/Fe^{3+} ions were co-precipitated in situ to induce magnetic feature to FV particles. Solutions contaminated with the model cationic dyes, methylene blue (MB) and crystal violet (CV), were treated by employing m-FV particles. Study on time of dyes removal showed a fast removing rate of MB and CV, reaching equilibrium at 10 and 5 minutes, respectively. Analysis of experimental kinetic data by the pseudo-first-order and pseudo-second-order models indicated a well-describing of data by the pseudo-second-order model. The isotherm data of adsorption of both cationic dyes on m-FV were modeled and revealed a well-describing with the Langmuir model. According to the Langmuir model, maximum adsorption capacities of 577 mg/g for MB and 1062 mg/g for CV on m-FV were observed. Easy recovery, good recyclability, pH-independent property, as well as the high capability in the removal of cationic dyes, the m-FV can be considered an effective and eco-friendly bio adsorbent in the treatment of dye contaminated solutions.

Keywords: *Adsorption; Crystal violet; Magnetic Fucus vesiculosus; Methylene blue*

How to cite this article
JafariH., Mahdavinia GR., Kazemi HeraghB., Javanshir Sh., Alinavaz S. Basic Dyes Removal by Adsorption Process Using Magnetic Fucus Vesiculosus (Brown Algae). J. Water Environ. Nanotechnol., 2020; 5(3): 256-269.
DOI: 10.22090/jwent.2020.03.006

INTRODUCTION

Today finding the effective and economical methods to remove dye pollution from wastewater as a significant environmental problem poses a major challenge to the industrial and scientific society [1,2]. Many attempts including biological, chemical, and physical methods have been employed to treat industrial wastewaters [3-5]. High efficiency, easy and secure handling and regeneration, low cost, and variety of adsorbents make the adsorption process attractive to remove toxic organic dyes produced by both dye manufacturing and dyeing industries [6-9]. Biosorption is a process that removes the pollution from wastewater by utilizing the biomass. Biological and natural materials such as polysaccharides, clays, and their nanocomposites, have been recently extended widely as biosorbent due to their accessible resources, inexpensive, and non-toxicity features [7,10,11]. Presence of active functional groups such as primary amine groups ($-NH_2$, chitosan), anionic carboxylate ($-CO_2^-$, alginate and carboxymethyl cellulose), and anionic sulfate ($-OSO_3^-$, *kappa*-carrageenan) make the polysaccharides as the satisfy candidates in the

* Corresponding Author Email: *grmnia@maragheh.ac.ir*

designing of adsorbents with excellent ability in the treatment of the dye contaminated effluents (mechanistically by entrapping the toxic ingredients electrostatically and physically) [2,12-18]. Because of their unique surface structures and high binding affinity (presence of some ingredients with active functional groups in their backbone), algae have high capacity as biosorbent. Although there are many kinds of algae, a few of them are investigated as biosorbent [19-21]. *Fucus vesiculosus* (FV) is a brown alga, abundant in see resources, with high fucoidan content, which in this study has been identified to be capable of removing toxic cationic dyes. Fucoidan, a natural sulfated polysaccharide, contains anionic sulfate ($-OSO_3^-$) and hydroxy (-OH) functional groups, making it feasible to bind or coordinate to cationic components [22]. The separation of alga after the adsorption process is difficult owing to their colloidal property. A combination of biosorbents with magnetic particles is a valid route that regardless of size can facilitate the recovery of biosorbent from media by applying the external magnetic field [23-31]. It should be noted that the use of synthetic adsorbents, including polymeric adsorbents, always has environmental problems. For example, in addition to the non-biodegradability of these materials, the diffusion of remained monomers in synthetic polymeric adsorbent may be led to secondary contamination [32]. Thus, using natural-based adsorbents is the demand of the industry to reduce environmental issues.

The main anionic compounds used as adsorbents contain carboxylate groups with a pK_a value of ~4.5, leading to the low adsorption capacity of cationic dyes at acidic media by the carboxylate-incorporated adsorbents [33]. Although this behavior may be helped the recovery of adsorbents at acidic media, the removal of cationic dyes from acidic wastewater could occur weakly. According to our previous work, using kappa-carrageenan (a biopolymer with sulfate groups) the removal of cationic dyes takes place in a wide range of pHs [25]. In fact, the removal of dyes by carrageenan-based adsorbents were not pH-dependent. Similar to carrageenan, the *Fucus vesiculosus* contains sulfate groups. Carrageenan-based adsorbents have been widely studied; whereas, the *Fucus vesiculosus* has not been investigated as an adsorbent in removal of cationic dyes. The main idea of this work was to evaluate the performance of *Fucus vesiculosus* as an adsorbent in removal of cationic dyes. Also, the effort was to evaluate the effect of pH on the adsorption of cationic dyes methylene blue and crystal violet on *Fucus vesiculosus* containing anionic sulfate groups.

Objectively, a novel magnetic *Fucus vesiculosus* (m-FV) bio adsorbent with a high adsorption capacity for cationic dyes was fabricated. A simple route processed it included co-precipitation of Fe^{2+}/Fe^{3+} ions-loaded brown algae via *in situ* approach. The preparation of the highly effective nanostructured composite to achieve particular dispersion is critical. To attain a magnetic bio adsorbent with high performance, the m-FV nanoparticles were treated using ultrasonic and freezing-drying techniques. The ultrasonic treatment induces the high-dispersed composite formation by applying acoustic cavitation during the process. It has great interest due to enhance the mixing feature and properties of materials [34]. The characteristic properties of the magnetic biosorbent, m-FV, including magnetic feature, surface morphology, crystallinity, and morphology of magnetite nanoparticles were investigated according to the related techniques. The magnetic bio adsorbent was employed to remove two different cationic dyes, methylene blue, and crystal violet, from their solutions. Crystal violet (CV) and methylene blue are synthetic and cationic dyes that transmit violet and blue colors in aqueous solutions. They are widely used in the textile industry for dyeing cotton, wool, silk, nylon, in the production of printing inks, as well as a biological stain, in veterinary medicine. The CV and MB are toxic and may be absorbed through the skin causing irritating and are harmful by inhalation and ingestion. In severe cases, can lead to kidney failure, severe eye irritation leading to permanent blindness and cancer [33]. The variation in the dye adsorption capacity of m-FV biosorbent was determined by changing of pH of MB and CV solutions, contact time, initial MB and CV concentrations, and ionic strength.

MATERIALS AND METHODS

Materials

Finlandia Pharmacy provided Fucus vesiculosus. Iron salts, $FeCl_3.6H_2O$ and $FeCl_2.4H_2O$, were obtained from Merck, Germany. Ammonia solution, methylene blue, and crystal violet were in analytical grade (Merck Co., Germany), and purification was not used.

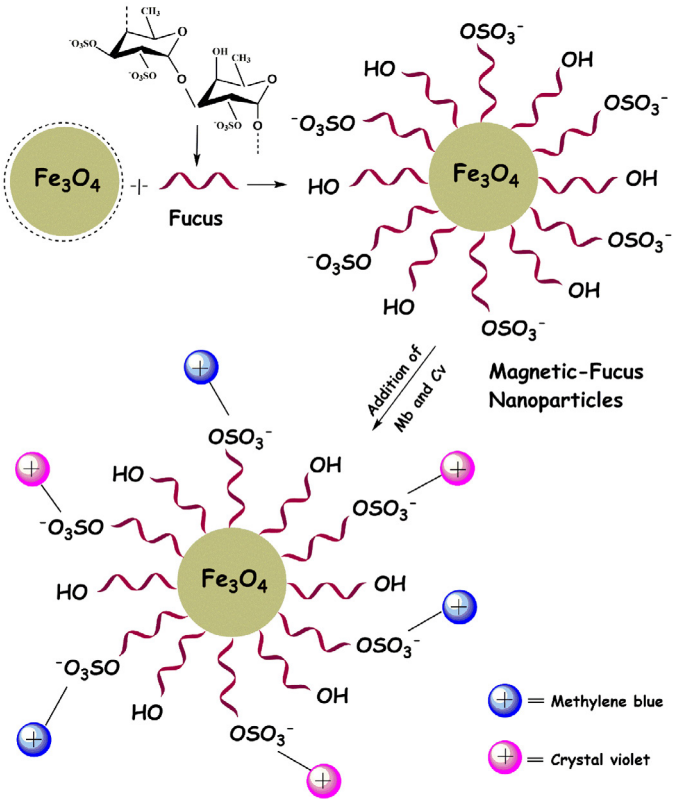

Fig. 1. A simple scheme showing the used steps for preparing magnetic FV nanoparticles.

Preparation of magnetic Brown Algae nanoparticles

The procedure used to prepare magnetic FV nanoparticles was according to our previous work [35]. The synthesis route of m-FV is shown in Fig. 1.

To achieve a dispersed FV, 2 g of its powder was poured in distilled water (200 mL), allowing to sonicate for 25 min (operating frequency: 50 kHz). After adjusting the temperature of the dispersed solution at 70 °C, separately, 3 g of $FeCl_3.6H_2O$ and 1.54g $FeSO_4.7H_2O$ was dissolved in 25 mL of distilled water and subsequently, their solution was poured into dispersed FV solution. After bubbling by N_2 gas for 30 min, diluted ammonia solution (3M) was slowly dropped into solution while stirring at 70 °C. The addition of ammonia solution was continued until the pH of the solution reached 10. A solution with a dark appearance was obtained that showing the formation of m-FV nanocomposite. The dark solution that its pH and temperature have been adjusted to 10 and 70 °C respectively, was stirred for 60 min. To remove any unreacted ingredients and alkali the produced m-FV nanoparticles were purified with excess distilled water. By reaching the pH of media to 7, the m-FV nanoparticles were magnetically collected by a magnet and treated by the freeze-drying process for 48 h to obtain porous m-FV nanoparticles.

Dye adsorption measurements

A batch method [36], as a common approach in dye removal experiments, was used to evaluate the performance of m-FV in the removal of MB and CV dyes. All experiments were done at 18 °C on a shaker while its speed was adjusted at 125 rpm. One hundred mg of magnetic bio adsorbent was immersed into 25 mL of MB and CV solutions (300 $mg.L^{-1}$). The kinetic study of the dye adsorption process was investigated by measuring the contents of MB and CV concentrations at different time intervals by using a UV-vis spectrometer (Shimadzu UV-1800; Japan) (λ= 664 and 590 nm for MB and CV, respectively). The Eq. 1 showed below can be applied to measure the amounts of dyes adsorbed on the bio adsorbent (q_t, $mg.g^{-1}$) at different times [37]:

$$q_t = \frac{(C_0 - C_t)}{m} \times V \quad (1)$$

where, initial concentrations of MB and CV dyes and their remained contents at time *t*, the volume of used dye solutions as well as the weight of m-FV biosorbent were shown as C_o (mg/L), and C_e (mg/L), *V* (L) and *m* (g), respectively. Twenty five mL of solutions containing MB or CV dyes with concentrations of 10, 25, 50, 100, 200, 300, 500, 1000, 2000, 3000, and 4000 mg.L^{-1} were used for isotherm studies (T= 18 °C, *m*=100 mg, t=24 h). The adsorption capacity of m-FV for both model dyes MB and CV at equilibrium time (24 h) was calculated using Eq. 1, which the C_t can be replaced with C_e (mg/L), showing equilibrium adsorption capacity of m-FV for MB and CV dyes. The pH of 25 mL of both CV and MB dyes (300 mg/L) was set at desired pHs by adding dilute solutions of 0.1 M of HCl or NaOH and the variation in adsorption capacity of m-FV for both dyes was determined (*m* of m-FV=100 mg, T=18 °C). To obtain thermodynamic parameters, adsorption processes were done at three temperatures (273, 298, and 313 K). The desired amount of NaCl (0.01-0.5 M in 25 mL of dyes aqueous solutions) was used to adjust the ionic strength to observe the changes in the dye adsorption process (*m* of m-FV=100 mg, T=18 °C, 300 mg/L of dyes). All experiments were done three times and the mean±SD were shown in figures.

Desorption studies

The desorption process was examined using different solutions [25], including acetic acid solution with 0.2 M of concentration, 0.5 M of KCl aqueous solution, and water-ethanol mixture with equal volume fraction as well as its 0.5 M of KCl water/ethanol solution. After the adsorption process, m-FV nanoparticles were collected magnetically and washed with distilled water to transfer any unabsorbed MB and CV dyes in water. By dispersing the CV- and MB-loaded m-FV nanoparticles into the mentioned desorption solutions and shaking them for 24 h, the concentrations of desorbed MB and CV dyes were determined according to the corresponding calibration curves. All experiments were done three times and the mean±SD were shown in figures.

Instrumentations

The image of magnetic nanoparticles was recorded with the help of transmission electron microscopy (TEM; Philips CM10 operating at 60 kV tension). After the coating of dried m-FV nanoparticles and non-magnetic FV with a thin layer of gold, the surface morphology of both samples was studied by using a scanning electron microscopy energy dispersive X-ray instrument (SEM/EDX, VEGAII, XMU, Czech Republic). Powder X-ray diffraction (XRD) patterns of FV and m-FV were obtained on a Siemens D-500 X-ray diffractometer (λ=1.54 Å (CuKα); current of 30 mA; voltage of 35 kV). The magnetic properties of m-FV nanoparticles were investigated using a vibrating sample magnetometer (VSM; model 7400, Lakeshare Company, USA). Dried and powdered raw materials and products were pelleted with dried KBr, and Fourier transform infrared (FT-IR) spectra were recorded using a Bruker 113V FT-IR spectrometer.

RESULT AND DISCUSSION

Synthesis and characterization

A new magnetic biosorbent with high performance to remove MB and CV cationic dyes were synthesized. Without introducing any toxic ingredient, the m-FV was prepared through a simple and green approach. (Fe^{2+}/Fe^{3+})-loaded FV dispersion was treated by ammonia solution, which resulting co-precipitation of iron ions via in situ to produce immobilized Fe_3O_4 on FV. Electrostatically interactions between Fe^{3+}/Fe^{2+} cations and the sulfate anions on the fucoidan may result in crosslinking and, consequently producing immobilized magnetic nanoparticles on FV particles [38,39]. The prepared magnetic FV was dried by using the freeze-drying process that causes increasing the accessible active centers in magnetic biosorbent by inducing a porous structure and, therefore lead to an increased surface area [40]. The structural characterization of m-FV biosorbent was investigated using common techniques, including FTIR, XRD, SEM, TEM, and VSM.

FTIR spectroscopy, XRD, and VSM study

To analyze the functional groups on raw materials and fabricated m-FV nanocomposite as well as chemical/physical interactions, the FTIR spectra were recorded and investigated (Fig. 2a). In the raw FV spectrum, 3429 cm^{-1} showed the presence of –OH groups, 1037 cm^{-1} attributed to secondary vibration of C-O in C-O-H groups, and 1265 and 825 cm^{-1} attributed to S=O (asymmetric stretching and stretching, respectively). The m-FV spectrum was similar to the raw FV spectrum with the small shift, verified the presence of FV, and revealed a sharp peak at 511 cm^{-1} can be

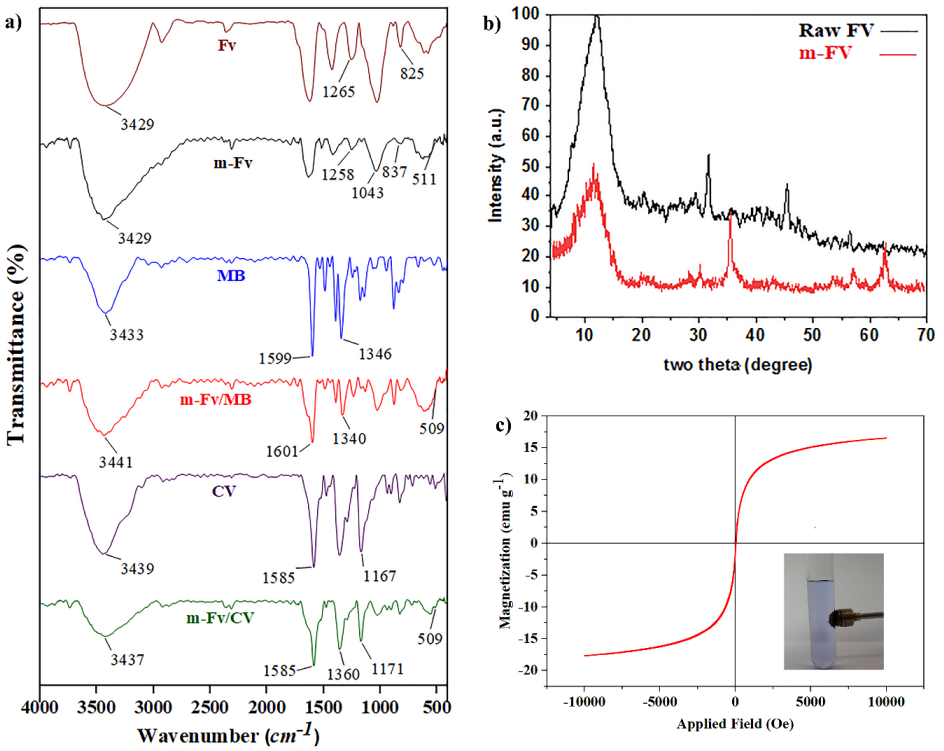

Fig. 2. (a) FTIR spectra of raw materials and products; (b) XRD patterns of raw FV and m-FV; (c) VSM curve of m-FV.

allotted to the stretching of Fe-O bond in Fe_3O_4 nanoparticles. The presence of all MB sharp bands: 1599 cm^{-1} corresponds to the C=N and C=C and 1346 cm^{-1} correspond to the C-N groups verified the adsorption of MB into m-FV. Also, the presence of all CV sharp bands: 1167 cm^{-1} corresponds to the C-N, 1585 cm^{-1} attributed to C=C in the benzene ring, and two bands (3439 and 3097 cm^{-1}) allot to N–H, verified the adsorption of CV into m-FV. However, there were shifting at some peaks for FTIR spectra of both MB and CV adsorbed on m-FV comparing to pure m-FV. The shifting at -OH stretching frequency indicated hydrogen bond formation between m-FV and MB/CV. Furthermore, the interaction between sulfate groups in m-FV and ammonium group in MB or CV confirmed by S=O asymmetric stretching and stretching frequencies shifting.

XRD patterns of m-FV and raw FV were illustrated in (Fig. 2b). The distinctive diffraction peaks of raw FV, 2θ = 12.3, and 31.66°, correspond to the partial crystalline structure of FV [38, 39]. The data are similar to the reported XRD analysis of fucoidan and water-soluble polysaccharides. The diffraction peaks of immobilized magnetic nanoparticles on the FV were appeared at 2θ= 30.4, 35.8, 43.4, 53.8, 57.3, and 63.1° (related to magnetic nanoparticles), indicating their corresponding indices (220), (311), (400), (422), (511), and (440), respectively. Bragg's equation (Eq. 2) was used to calculating the interplanar distances [41]:

$$n\lambda=2d\sin\theta \quad (2)$$

where λ is the incident X-ray wavelength of Cu-Kα, θ is incident angle i.e. angle between the incident ray and scatter plane, d is the spacing of the crystal layers (path difference) and n is a positive integer. The interplanar distances found to be 2.94 Å (2θ=30.4°), 2.523 Å (2θ=35.6°), 2.086 Å (2θ=43.4°), 1.702 Å (2θ=53.8°), 1.606 Å (2θ=57.3°), and 1.606 Å (2θ=63°) for m-FV. The results are in agreement well with the database indexed in the JCPDS file (PDF No. 65-3107) [42]. The formation of pure magnetite with a spinel structure and high crystalline structure can be concluded from the results.

The hysteresis loop of m-FV was investigated at 298K using VSM, and the applied field was in the range of ±10 kOe (Fig. 2c). Owing to the nano-

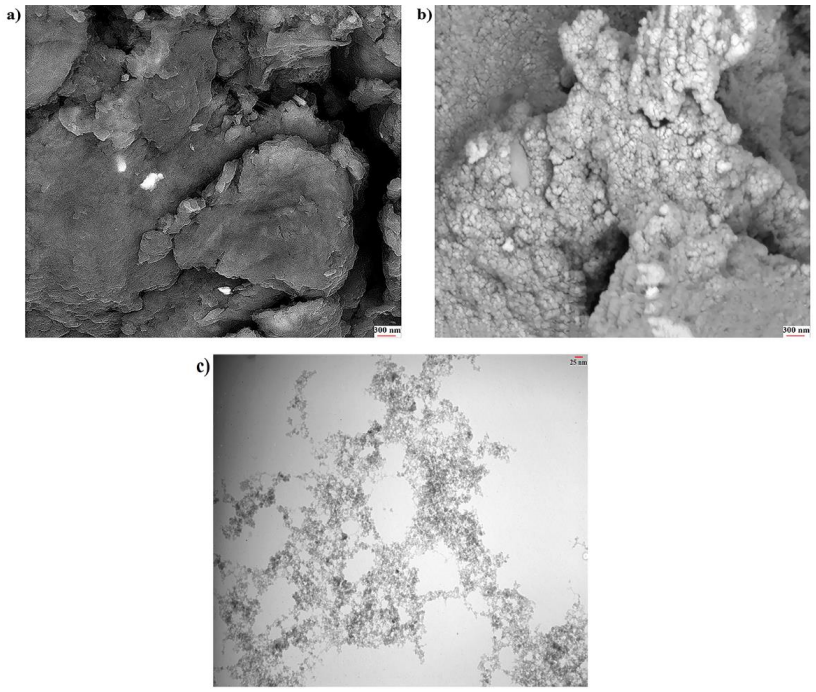

Fig. 3. SEM micrographs of (a) raw FV and (b) m-FV; (c) TEM image of m-FV.

scale size of immobilized magnetite (Fe_3O_4) on FV the m-FV sample showed superparamagnetic properties with no coercivity. Introducing the immobilized Fe_3O_4 nanoparticles on FV caused a saturation magnetization (Ms) of about 16.5 $emu.g^{-1}$. This reduction in Ms value can be assigned to the coating effect of FV on magnetite nanoparticles. Because of reporting the Ms value as per g of blended magnetite adsorbent, the Ms value is dependent on its weight ratio of Fe_3O_4 in the m-FV composition, and its blending with FV causes a reduction in Ms value. However, the magnetic saturation of m-FV biosorbent was sufficient to separate it from the treated dyes solutions upon applying an external magnet.

SEM and TEM studies

The surface morphologies of FV and m-FV were studied, and a significant difference was observed due to the immobilized Fe_3O_4 nanoparticles on the surface morphology of FV. The SEM images of FV and m-FV were shown in Fig. 3(a) and (b). As shown in figures, there is a clear difference between SEM images of FV and m-FV. Raw FV showed a smooth and homogenous surface morphology. While, it was rough and uneven for m-FV, which indicates the attaching of Fe_3O_4 nanoparticles to the surface of FV. The TEM image (Fig. 3(c)) showed a nanoporous structure and well-dispersed Fe_3O_4 particles with a distribution of particle size less than 25 nm.

Dye adsorption study

Effect of pH and ionic strength on the adsorption

Among many factors, the pH and ionic strength of dye wastewater can influence the adsorption capacity of bioadsorbents, which depend on their nature. The adsorption of polysaccharides with anionic functional groups, mechanistically with electrical adsorption specifics, influence by ion strength through the neutralization of anionic groups with cations [43]. The effect of ionic strength on dye adsorption capacity of m-FV, which contains fucoidan as the most ingredient with active $^{-}OSO_3^{-}$ groups, was tested using NaCl solutions at 0.01-0.5 M concentration ranges. As expected, the result revealed a gradual decrease in MB and a slight decrease in CV adsorption capacity of magnetic biosorbent, with increasing the NaCl concentration (Fig. 4(a)). This reduction can be attributed to the competition between Na^+ ions and cationic ammonium groups of MB and CV to adsorb on bioadsorbents [44]. The higher mobility of Na^+ than the MB or CV molecules due to the smaller size of Na^+ (1.02 Å) ingredient toward MB (15.06 Å) and CV (14.52 Å), therefore,

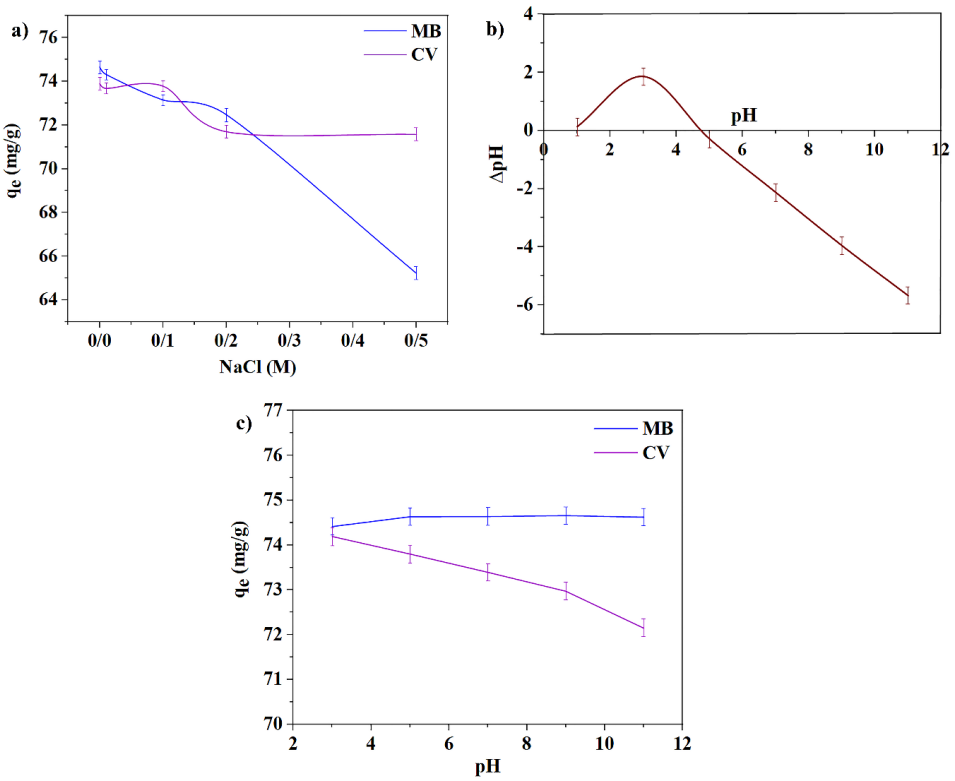

Fig. 4. (a) Effect of NaCl concentration on adsorption capacity of m-FV for MB and CV; (b) Points zero charge plot of m-FV for determination pHpzc; (c) Effect of initial the pH of MB and CV solutions on adsorption capacity of m-FV for MB and CV (25 mL of 300 mg.g^{-1} of MB; adsorbent dosage: 25 mg; room temperature).

the Na^+ cations is more accessible than that of both MB and CV molecules to adsorb on the surface of m-FV [45]. Besides, the sulfate groups on the bioadsorbent maybe shield by the Na^+ ions, which prevents the approaching cationic MB and CV dyes on the adsorbent. Indeed, decreasing in adsorption capacity by increasing the ionic strength of solution can be originated from the repulsive force between Na^+ and cationic MB and CV dyes [43].

The initial pH of dyes solutions not only effects the surface charge of bioadsorbent, but also the degree of ionization of dyes can be altered. To investigate the variation in the adsorption process by changing the pH of dyes solutions, the points zero charges (pHpzc) of magnetic biosorbent, which is an essential factor, must first be determined. Generally, the cationic adsorbate tends to adsorb on adsorbent at pH>pHpzc; whereas, adsorption takes place for anionic adsorbate at pH<pHpzc [46]. The pHpzc of m-FV was found to be in a range of 2.6-3.0 (Fig. 4(b)). Therefore, the pH-dependency of the adsorption behavior was studied by altering the pHs of CV and MB pollutions in a range of 3-9. As can be concluded from the data (Fig. 4(c)), the magnetic FV showed insufficient sensitivity to the pH of both MB and CV solutions. It may be noted that in the wide range of pHs, the ammonium pendants on both CV and MB dyes exist in the cationic form. Also, the high dissociation behavior of $-OSO_3^-$ groups on FV makes the m-FV as a pH-independent bioadsorbent, which exists in the anionic form at pH>3 [45].

Kinetic of adsorption

Kinetics of pollution removing, an important parameter in the adsorption processes can affect the efficiency of dye removing processes. The high rate removing of pollution, moreover than capacity, makes an adsorbent eligible. The required time to reach the equilibrium of adsorption of MB and CV on m-FV the effect of contact time was studied. According to the results from kinetics curves of adsorption processes (Fig. 5 (a) and (b)), the removing of both MB and CV dyes were too fast and reached to equilibrium at 10 and 5 minutes, respectively by fitting the experimental

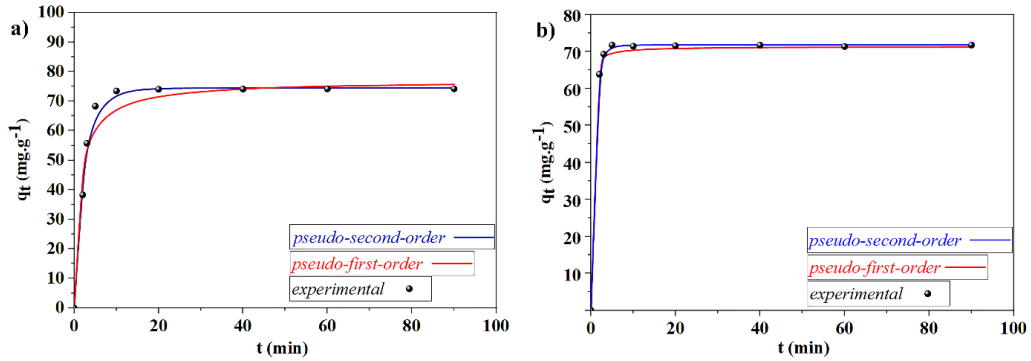

Fig. 5. Modeling of adsorption kinetics of dye removal according to pseudo-first-order and pseudo-second-order models by m-FV for (a) MB, (b) CV.

Table 1. Kinetic parameters of adsorption of MB and CV onto m-FV calculated according to kinetic models.

	pseudo-first-order			pseudo-second-order			
	K_1 (min^{-1})	q_e ($mg.g^{-1}$)	r^2	$K_2\times10^3$ ($g.min^{-1}.mg^{-1}$)	q_e ($mg.g^{-1}$)	r^2	$q_{e.exp}$ ($mg.g^{-1}$)
MB	0.423	73.46	0.8681	10.31	74.46	0.9763	74.65
CV	1.106	75.77	0.9493	121.6	76.41	0.9843	76.88

data to the pseudo-second-order and pseudo-first-order kinetic models, the related parameters were calculated, and the results are demonstrated in Table 1. The applied kinetic models that were shown in Eqs 2 and 3 represent the pseudo-first-order model and pseudo-second-order model, respectively [47]:

$$q_t = q_e\left(1-e^{k_1 t}\right) \quad (2)$$

$$q_t = \frac{q_e^{\,2} k_2 t}{1+q_e k_2 t} \quad (3)$$

where, q_e and q_t ($mg.g^{-1}$) are related to the amounts of the MB and CV dyes adsorbed on the m-FV bioadsorbent at the equilibrium and at the desired time t, respectively. k_1 (min^{-1}) and k_2 ($g.mg^{-1}.min^{-1}$) are the rate constants of pseudo-first-order kinetic pseudo-second-order kinetic models. As illustrated in Table 1 and Figs. 5, among two kinetic models investigated, the pseudo-second-order kinetic model revealed the best fit for adsorption of both MB (0.9763) and CV (0.9843) on m-FV bioadsorbent. Moreover, the theoretical adsorption capacity of m-FV for MB and CV calculated according to pseudo-second-order model (q_e) were obtained 74.46 and 76.41 $mg.g^{-1}$ for MB and CV, respectively, and were relatively in good agreement with the experimental ones ($q_{e.exp}$ = 74.64 and 76.88 $mg.g^{-1}$ for MB and CV, respectively).

Adsorption isotherms

The effect of initial dyes concentrations on the adsorption behavior of m-FV was investigated to explain the type of molecular distribution of MB and CV pollutions on the m-FV using two common isotherm models, Langmuir and Freundlich (Fig. 6 (a) and (b)). Firstly, a clear enhancing in the adsorption capacity of m-FV for both MB and CV could be observed by the increase in the initial concentration of both MB and CV. Afterward, because of reaching the saturation state of the adsorption sites on m-FV the adsorption begins to level off and, subsequently, the adsorption capacity of m-FV for both dyes tends to remain constant. To predict the extent of maximum adsorption capacity of m-FV, as well as the type of molecular distribution of MB and CV pollutions on the m-FV the experimental data, were fitted to the Langmuir and Freundlich models. For Langmuir model, monolayer adsorption of dyes onto the bioadsorbent is assumed, and the adsorption of MB and CV takes place at structurally homogeneous sites of m-FV. In contrast, in the Freundlich one, the adsorption of pollutants onto the adsorbent is based on the adsorption of dyes on the heterogeneous sites of adsorbent with a multilayer adsorption process.

The mathematical expressions of nonlinear Langmuir (Eq. 4) and Freundlich (Eq. 5) models, as well as the R_L (Eq. 6) dimensionless constant of

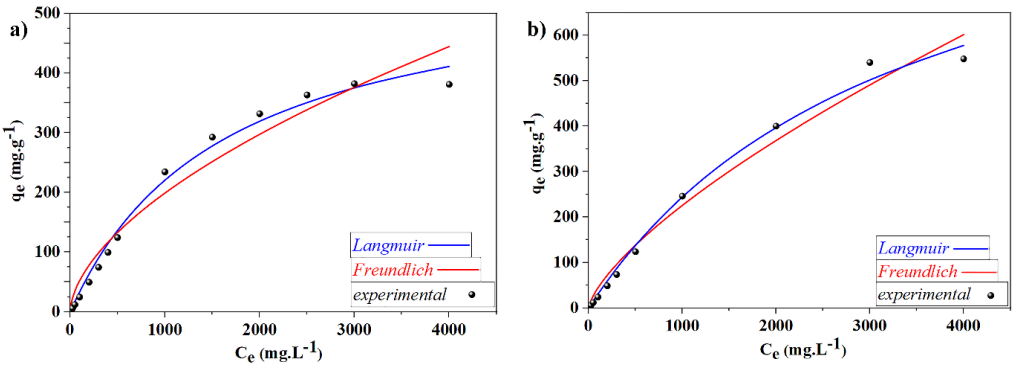

Fig. 6 Modeling of adsorption isotherms by applying Langmuir and Freundlich models for removal of (a) MB and (b) CV by m-FV (Time 60 h; Adsorbent dosage: 0.025 mg; Volume of MB and CV solutions: 25 mL; room temperature).

Table 2. Estimated isotherm parameters determined according to the Langmuir and Freundlich models for the adsorption of MB and CV onto m-FV.

	Freundlich			Langmuir			
	n	K_F $(mg.g^{-1})(g.L^{-1})^{-1/n}$	r^2	q_m $(mg.g^{-1})$	K_L $(L.g^{-1})$	r^2	R_L $(mg.g^{-1})$
MB	1.725	3.628	0.9595	577.1	0.000619	0.9914	0.9986
CV	1.415	1.713	0.9811	1062	0.000298	0.9937	0.9993

adsorption obtaining from Langmuir model, are presented as below [47]:

$$q_e = \frac{q_m K_L C_e}{1 + K_L C_e} \quad (4)$$

$$q_e = k_f C_e^{1/n} \quad (5)$$

$$R_L = \frac{1}{1 + K_L C_0} \quad (6)$$

where the concentrations of MB and CV in the solution and adsorption capacity at equilibrium time were shown as Ce (mg L^{-1}) and qe (mg g^{-1}). K_L (L mg^{-1}) and k_F (mg g^{-1})(Lmg^{-1})$^{1/n}$ are the isotherm constants of Langmuir and Freundlich models, respectively; and the theoretically maximum adsorption capacity (q_m, mg g^{-1}) and empirical constant, 1/n, can be calculated from corresponding models. The results were indicated in Fig. 6 and all data calculated according to the mentioned models were illustrated in Table 2. As is clear from curves and correlation coefficients (r2>0.99), the experimental isotherm data in this work were in good agreement with the Langmuir than that of the Freundlich model, which demonstrate a homogeneous adsorption process through monolayer distribution onto the surface of the m-FV adsorbent. Besides, the R_L values, indicating the type of isotherm, were determined from the Langmuir model and were found to be between 0 and 1 for both MB and CV adsorption process, representing a favorable adsorption system. The R_L values of 0-1 ($0 < R_L < 1$) is favorable, while $R_L > 1$ is unfavorable; $R_L = 1$, linear condition; and $R_L = 0$ is irreversible condition [48].

Thermodynamic studies

The influence of temperature on the adsorption behavior of MB and CV pollutants onto the m-FV was investigated at three temperatures to obtain thermodynamic parameters. The thermodynamic parameters, including enthalpy change (ΔH, kJ/mol), entropy change (ΔS, J/(K mol), and standard Gibbs free energy (ΔG, kJ/mol) can provide important information regarding the energy changes of the adsorption process of pollutants on adsorbents. The thermodynamic parameters mentioned above could be calculated by the following equations [49, 50]:

$$K_c = \frac{C_s}{C_e} \quad (7)$$

$$LnK_c = -\frac{\Delta H}{RT} + \frac{\Delta S}{R} \quad (8)$$

$$\Delta G = \Delta H - T\Delta S \quad (9)$$

where, *Kc*, the equilibrium constant, is calculated

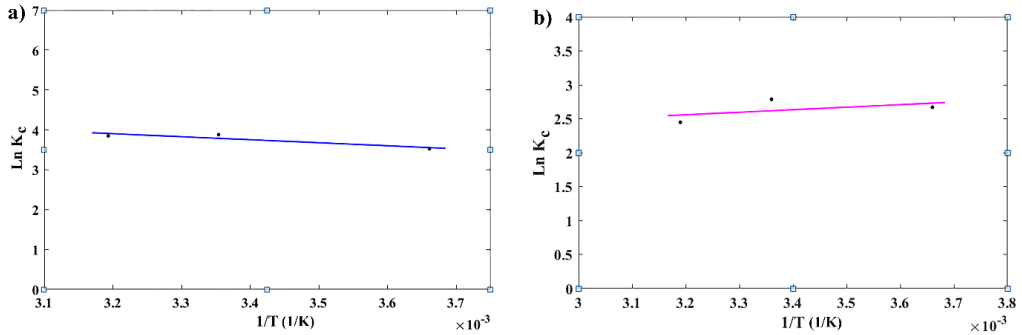

Fig. 7. The plot of lnK vs. 1/T for the estimation of the thermodynamic parameters for the adsorption of (a) MB and (b) CV on m-FV.

Table 3. Calculated thermodynamic parameters for the removal of MB and CV by m-FV at different temperatures.

	T (K)	ΔG (J.mol^{-1})	ΔH (J.mol^{-1})	ΔS (J.K^{-1}.mol^{-1})
	273	-8065.6		
MB	298	-9379.86	6286	52.57
	313	-10168.41		
	273	-6197.74		
CV	298	-6482.24	-3091	11.38
	313	-6652.94		

from the C_s and C_e, the concentrations of MB, and CV on m-FV and in solutions, respectively. *R* and *T* are the universal gas constant (8.314 J mol K^{-1}) and absolute temperature in Kelvin (K), respectively. The *LnKc* versus *1/T* (Fig. 7 (a) and (b)) gives a linear plot that the *ΔH* and *ΔS* can be obtained from the slope and intercept of the obtained plot. The calculated data were summarized in Table 3. According to the obtained data, the endothermic specific was indicated for the process of MB adsorption on m-FV due to the positive value of *ΔH*, at the same time it was exothermic for CV due to the negative value of *ΔH*. However, *ΔG* for the adsorption processes of both MB and CV on m-FV was negative that revealed their feasibility and spontaneous natures. Moreover, increasing the negative value of *ΔG* with increasing temperature were revealed the adsorption dependency on temperature that offers increasing tendency at the feasibility and spontaneously of adsorption processes with increasing temperature. The *ΔS* values were positive for both MB and CV adsorption processes that suggest an increase in disorder and randomness at the solid/solution interface.

Desorption study and mechanism of adsorption

Not only the high adsorption capacity of adsorbents plays a significant role in the removal of pollutions, but the recyclability of adsorbent is also very important in economic, which reusing the adsorbent with more cycles, take low-cost processes. Considering the reusability importance, the experimental examination carried out by desorbing tests of MB and CV from m-FV in different solutions: ethanol, ethanol/water (50:50, V: V), acetic acid 0.2 M, KCl 0.5 M, and KCl 0.05 M in ethanol/water (50:50, V: V). The results are presented in Figs. 8 (a), (b), (c) and (d). The KCl in ethanol/water found out to be a suitable solution for recycling both MB and CV dyes by 97.5 and 96 % desorption contents, respectively. The results are consistent with decreasing adsorption of m-FV by increasing ionic strength, the studies discussed above. On the other hand, the interaction of anionic sulfate groups with K^+ ions are preferred than that of cationic dyes. The interaction between sulfate groups of carrageenan with K^+ ions which is similar to FV structurally has been reported [51]. It shows good desorption behavior for dyes in both KCl and ethanol solutions, but it was not sufficient. Therefore, enhancing ethanol solution to KCl solution increased the desorption of dyes, remarkable. The experimental tests also did not show desorption at the acetic acid media (only about 2 % for both MB and CV), which is compatible with pH independence of biosorbent, the results obtained in the pH studies. In fact, the low pKa value of sulfate groups on FV favors the dissociation of these

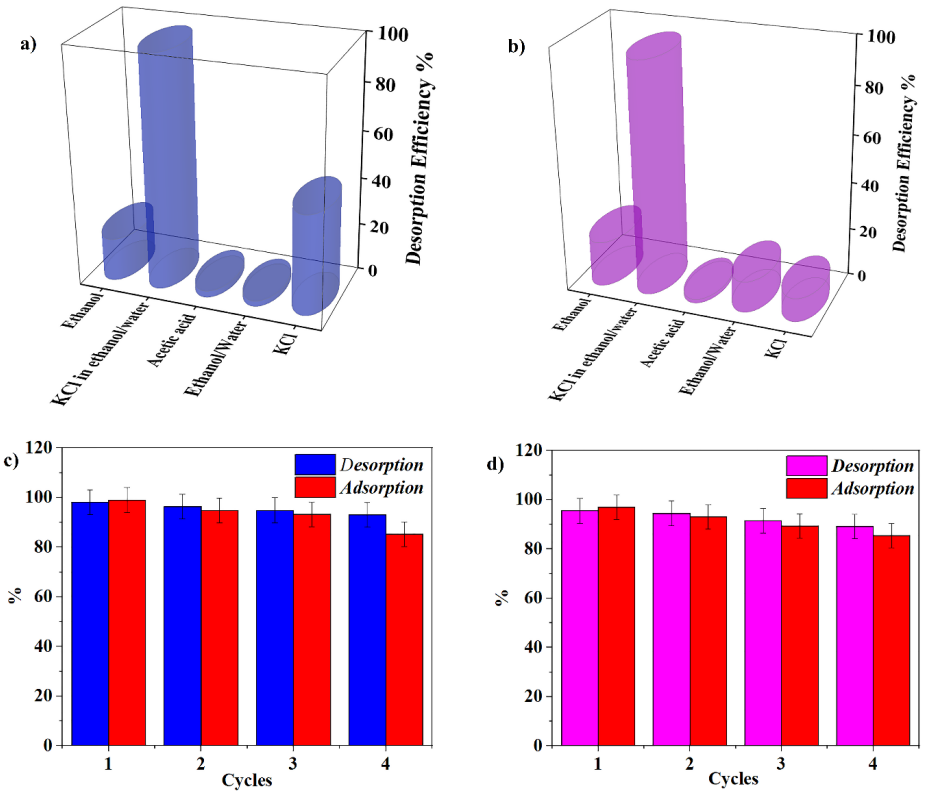

Fig. 8. Desorption efficiency of (a) MB and (b) CV from m-FV by various solutions; Adsorption-desorption of (c) MB and (d) CV from m-FV using 0.1 M KCl (ethanol: H_2O 50:50) for 4 cycles.

Table 4 Different adsorbents used to remove the MB and CV dyes

Dye	Adsorbent	Adsorption capacity ($mg.g^{-1}$)	Reference
Methylene blue	Bamboo based activated carbon	454	[55]
Methylene blue	Coconut shell activated carbon	277	[55]
Methylene blue	Rice husk activated carbon	343	[55]
Methylene blue	magnetic polyvinyl alcohol/laponite RD	251	[28]
Methylene blue	Jute fiber carbon	225	[56]
Methylene blue	Magnetic Fucus vesiculosus	577.1	Present work
Crystal Violet	OC-BzM nanoparticles	248	[57]
Crystal Violet	CarAlg/MMt nanocomposite Hydrogel	88	[17]
Crystal Violet	Nanomagnetic iron oxide	16	[58]
	Magnetically modified		

anionic groups in a wide range of pHs. As a result, it has no tendency to protonate in the presence of acid [25]. The adsorbent recyclability was verified by four adsorption-desorption cycles with a little decrease at adsorption capacity (about 6 % for both MB and CV) at the mentioned conditions. Given its good adsorption capacity and recyclability, the m-FV bioadsorbent can be considered as a proper candidate in removing cationic dyes from contaminated solutions (Table 4). The mechanism of the adsorption processes predicted using the results of the FTIR spectrum, pH effect, and ionic

strength as well as from adsorption-desorption studies of biosorbent. According to the results, in addition to weak interactions involve Van der Waals forces and hydrogen bonds [52], electrostatic interactions between anionic sulfate groups and cationic ammonium groups on dyes have made new magnetic biosorbent more effective comparing other adsorbents (Table 4). Hydrogen bond developments and electrostatic interactions were recognized through the shifting of the -OH and sulfate group frequencies after the MB and CV adsorption on the m-FV at the FTIR spectrum. pH insensitive behavior of m-BA demonstrated the mechanism of adsorption progression through sulfate group interaction. The sulfate group causes the magnetic biosorbent to exist in the anionic form at a wide range (pH>3). Furthermore, decreasing adsorption capacity by increasing the ionic strength of solutions confirmed the electrostatic interactions. The shielding effect of Na^+ on sulfate groups on bioadsorbent prevents the approaching of the cationic centers of dyes to the anionic centers of magnetic biosorbent.

CONCLUSION

A high effective magnetic biosorbent based on marine brown algae has been prepared and used for the effective removing cationic dye pollutants. The magnetic biosorbent, produced through a facile and green method, presented a fast and up to nearly 100 % removal specifics for MB and CV cationic dyes. The magnetic biosorbent showed a high adsorption capacity of 577, 1062 $mg.g^{-1}$ for MB and CV, respectively, and the high fast adsorption rate confirmed by the adsorption kinetics. The high efficiency of m-FV to remove cationic dyes assigned to the fucoidan ingredient carrying negatively charged centers as well as a porous structure of magnetic biosorbent. Improvement of the brown algae by magnetic nanoparticles to easy remove of biosorbent from wastewater and good recyclability made it more effective. These brilliant specifics and low-cost resources of biosorbent exhibit real potential for utilization in the industry.

CONFLICT OF INTEREST

Author declares no conflict of interest.

REFERENCES

1. Adegoke KA, Bello OS. Dye sequestration using agricultural wastes as adsorbents. Water Resources and Industry. 2015;12:8-24.
2. Karimi MH, Mahdavinia GR, Massoumi B, Baghban A, Saraei M. Ionically crosslinked magnetic chitosan/κ-carrageenan bioadsorbents for removal of anionic eriochrome black-T. International Journal of Biological Macromolecules. 2018;113:361-75.
3. Turhan K, Turgut Z. Decolorization of direct dye in textile wastewater by ozonization in a semi-batch bubble column reactor. Desalination. 2009;242(1-3):256-63.
4. Ghorai S, Sarkar A, Raoufi M, Panda AB, Schönherr H, Pal S. Enhanced Removal of Methylene Blue and Methyl Violet Dyes from Aqueous Solution Using a Nanocomposite of Hydrolyzed Polyacrylamide Grafted Xanthan Gum and Incorporated Nanosilica. ACS Applied Materials & Interfaces. 2014;6(7):4766-77.
5. Fakhru'l-Razi A, Pendashteh A, Abdullah LC, Biak DRA, Madaeni SS, Abidin ZZ. Review of technologies for oil and gas produced water treatment. Journal of Hazardous Materials. 2009;170(2-3):530-51.
6. Mu B, Wang A. Adsorption of dyes onto palygorskite and its composites: A review. Journal of Environmental Chemical Engineering. 2016;4(1):1274-94.
7. Gupta NK, Gupta A, Ramteke P, Sahoo H, Sengupta A. Biosorption-a green method for the preconcentration of rare earth elements (REEs) from waste solutions: A review. Journal of Molecular Liquids. 2019;274:148-64.
8. Sadasivam S, Krishna SK, Ponnusamy K, Nagarajan GS, Kang TW, Venkatesalu SC. Equilibrium and Thermodynamic Studies on the Adsorption of an Organophosphorous Pesticide onto "Waste" Jute Fiber Carbon. Journal of Chemical & Engineering Data. 2010;55(12):5658-62.
9. Shalla AH, Bhat MA, Yaseen Z. Hydrogels for removal of recalcitrant organic dyes: A conceptual overview. Journal of Environmental Chemical Engineering. 2018;6(5):5938-49.
10. Carvalho J, Araujo J, Castro F. Alternative Low-cost Adsorbent for Water and Wastewater Decontamination Derived from Eggshell Waste: An Overview. Waste and Biomass Valorization. 2011;2(2):157-67.
11. Crini G. Recent developments in polysaccharide-based materials used as adsorbents in wastewater treatment. Progress in Polymer Science. 2005;30(1):38-70.
12. Sui K, Li Y, Liu R, Zhang Y, Zhao X, Liang H, et al. Biocomposite fiber of calcium alginate/multi-walled carbon nanotubes with enhanced adsorption properties for ionic dyes. Carbohydrate Polymers. 2012;90(1):399-406.
13. Zirak M, Abdollahiyan A, Eftekhari-Sis B, Saraei M. Carboxymethyl cellulose coated Fe3O4@SiO2 core–shell magnetic nanoparticles for methylene blue removal: equilibrium, kinetic, and thermodynamic studies. Cellulose. 2017;25(1):503-15.
14. Mahdavinia GR, Karami S. Synthesis of magnetic carboxymethyl chitosan-g-poly(acrylamide)/laponite RD nanocomposites with enhanced dye adsorption capacity. Polymer Bulletin. 2015;72(9):2241-62.
15. Thakur VK, Thakur MK. Recent Advances in Graft Copolymerization and Applications of Chitosan: A Review. ACS Sustainable Chemistry & Engineering. 2014;2(12):2637-52.
16. Peng N, Hu D, Zeng J, Li Y, Liang L, Chang C. Superabsorbent Cellulose–Clay Nanocomposite Hydrogels for Highly Efficient Removal of Dye in Water. ACS Sustainable Chemistry & Engineering. 2016;4(12):7217-24.
17. Mahdavinia GR, Aghaie H, Sheykhloie H, Vardini MT, Etemadi H. Synthesis of CarAlg/MMt nanocomposite hydrogels and adsorption of cationic crystal violet. Carbohydrate Polymers. 2013;98(1):358-65.

18. Mahdavinia GR, Bazmizeynabad F, Seyyedi B. kappa-Carrageenan beads as new adsorbent to remove crystal violet dye from water: adsorption kinetics and isotherm. Desalination and Water Treatment. 2013;53(9):2529-39.
19. Negm NA, Abd El Wahed MG, Hassan ARA, Abou Kana MTH. Feasibility of metal adsorption using brown algae and fungi: Effect of biosorbents structure on adsorption isotherm and kinetics. Journal of Molecular Liquids. 2018;264:292-305.
20. Aravindhan R, Rao JR, Nair BU. Removal of basic yellow dye from aqueous solution by sorption on green alga Caulerpa scalpelliformis. Journal of Hazardous Materials. 2007;142(1-2):68-76.
21. Ata A, Nalcaci OO, Ovez B. Macro algae Gracilaria verrucosa as a biosorbent: A study of sorption mechanisms. Algal Research. 2012;1(2):194-204.
22. Chevolot L, Mulloy B, Ratiskol J, Foucault A, Colliec-Jouault S. A disaccharide repeat unit is the major structure in fucoidans from two species of brown algae. Carbohydrate Research. 2001;330(4):529-35.
23. Hosseini F, Sadighian S, Hosseini-Monfared H, Mahmoodi NM. Dye removal and kinetics of adsorption by magnetic chitosan nanoparticles. Desalination and Water Treatment. 2016;57(51):24378-86.
24. Liu K, Chen L, Huang L, Lai Y. Evaluation of ethylenediamine-modified nanofibrillated cellulose/chitosan composites on adsorption of cationic and anionic dyes from aqueous solution. Carbohydrate Polymers. 2016;151:1115-9.
25. Mahdavinia GR, Mosallanezhad A. Facile and green rout to prepare magnetic and chitosan-crosslinked κ-carrageenan bionanocomposites for removal of methylene blue. Journal of Water Process Engineering. 2016;10:143-55.
26. Bée A, Obeid L, Mbolantenaina R, Welschbillig M, Talbot D. Magnetic chitosan/clay beads: A magsorbent for the removal of cationic dye from water. Journal of Magnetism and Magnetic Materials. 2017;421:59-64.
27. Sivashankar R, Sathya AB, Vasantharaj K, Sivasubramanian V. Magnetic composite an environmental super adsorbent for dye sequestration – A review. Environmental Nanotechnology, Monitoring & Management. 2014;1-2:36-49.
28. Mahdavinia GR, Soleymani M, Sabzi M, Azimi H, Atlasi Z. Novel magnetic polyvinyl alcohol/laponite RD nanocomposite hydrogels for efficient removal of methylene blue. Journal of Environmental Chemical Engineering. 2017;5(3):2617-30.
29. Mola ali abasiyan S, Mahdavinia GR. Polyvinyl alcohol-based nanocomposite hydrogels containing magnetic laponite RD to remove cadmium. Environmental Science and Pollution Research. 2018;25(15):14977-88.
30. Rao P, Lo IMC, Yin K, Tang SCN. Removal of natural organic matter by cationic hydrogel with magnetic properties. Journal of Environmental Management. 2011;92(7):1690-5.
31. Dong C, Chen W, Liu C, Liu Y, Liu H. Synthesis of magnetic chitosan nanoparticle and its adsorption property for humic acid from aqueous solution. Colloids and Surfaces A: Physicochemical and Engineering Aspects. 2014;446:179-89.
32. Jamshidi A, Ahmad Khan Beigi F, Kabiri K, Zohuriaan-Mehr MJ. Optimized HPLC determination of residual monomer in hygienic SAP hydrogels. Polymer Testing. 2005;24(7):825-8.
33. Jana S, Ray J, Mondal B, Pradhan SS, Tripathy T. pH responsive adsorption/desorption studies of organic dyes from their aqueous solutions by katira gum-cl-poly(acrylic acid-co-N-vinyl imidazole) hydrogel. Colloids and Surfaces A: Physicochemical and Engineering Aspects. 2018;553:472-86.
34. Dehnad D, Emam-Djomeh Z, Mirzaei H, Jafari S-M, Dadashi S. Optimization of physical and mechanical properties for chitosan–nanocellulose biocomposites. Carbohydrate Polymers. 2014;105:222-8.
35. Soleymani M, Akbari A, Mahdavinia GR. Magnetic PVA/laponite RD hydrogel nanocomposites for adsorption of model protein BSA. Polymer Bulletin. 2018;76(5):2321-40.
36. Mahdavinia GR, Rahmani Z, Mosallanezhad A, Karami S, Shahriari M. Effect of magnetic laponite RD on swelling and dye adsorption behaviors of κ-carrageenan-based nanocomposite hydrogels. Desalination and Water Treatment. 2015;57(43):20582-96.
37. Ahlawat W, Kataria N, Dilbaghi N, Hassan AA, Kumar S, Kim K-H. Carbonaceous nanomaterials as effective and efficient platforms for removal of dyes from aqueous systems. Environmental Research. 2020;181:108904.
38. Jeong H-S, Venkatesan J, Kim S-K. Hydroxyapatite-fucoidan nanocomposites for bone tissue engineering. International Journal of Biological Macromolecules. 2013;57:138-41.
39. Saravana PS, Cho Y-J, Park Y-B, Woo H-C, Chun B-S. Structural, antioxidant, and emulsifying activities of fucoidan from Saccharina japonica using pressurized liquid extraction. Carbohydrate Polymers. 2016;153:518-25.
40. Jeddou KB, Chaari F, Maktouf S, Nouri-Ellouz O, Helbert CB, Ghorbel RE. Structural, functional, and antioxidant properties of water-soluble polysaccharides from potatoes peels. Food Chemistry. 2016;205:97-105.
41. El-Shamy AG. An efficient removal of methylene blue dye by adsorption onto carbon dot @ zinc peroxide embedded poly vinyl alcohol (PVA/CZnO2) nano-composite: A novel Reusable adsorbent. Polymer. 2020;202:122565.
42. Chen S, Duan J, Tang Y, Zhang Qiao S. Hybrid Hydrogels of Porous Graphene and Nickel Hydroxide as Advanced Supercapacitor Materials. Chemistry - A European Journal. 2013;19(22):7118-24.
43. Unuabonah EI, Olu-owolabi BI, Okoro D, Adebowale KO. Comparison of two-stage sorption design models for the removal of lead ions by polyvinyl-modified Kaolinite clay. Journal of Hazardous Materials. 2009;171(1-3):215-21.
44. Unuabonah EI, Taubert A. Clay–polymer nanocomposites (CPNs): Adsorbents of the future for water treatment. Applied Clay Science. 2014;99:83-92.
45. Macedo JdS, da Costa Júnior NB, Almeida LE, Vieira EFdS, Cestari AR, Gimenez IdF, et al. Kinetic and calorimetric study of the adsorption of dyes on mesoporous activated carbon prepared from coconut coir dust. Journal of Colloid and Interface Science. 2006;298(2):515-22.
46. Wang L, Zhang J, Wang A. Removal of methylene blue from aqueous solution using chitosan-g-poly(acrylic acid)/montmorillonite superadsorbent nanocomposite. Colloids and Surfaces A: Physicochemical and Engineering Aspects. 2008;322(1-3):47-53.
47. Dragan ES, Apopei Loghin DF, Cocarta AI. Efficient Sorption of Cu2+ by Composite Chelating Sorbents Based on Potato Starch-graft-Polyamidoxime Embedded in

Chitosan Beads. ACS Applied Materials & Interfaces. 2014;6(19):16577-92.
48. Pal S, Ghorai S, Das C, Samrat S, Ghosh A, Panda AB. Carboxymethyl Tamarind-g-poly(acrylamide)/Silica: A High Performance Hybrid Nanocomposite for Adsorption of Methylene Blue Dye. Industrial & Engineering Chemistry Research. 2012;51(48):15546-56.
49. Inthapanya X, Wu S, Han Z, Zeng G, Wu M, Yang C. Adsorptive removal of anionic dye using calcined oyster shells: isotherms, kinetics, and thermodynamics. Environmental Science and Pollution Research. 2019;26(6):5944-54.
50. Li Y, Zhang P, Du Q, Peng X, Liu T, Wang Z, et al. Adsorption of fluoride from aqueous solution by graphene. Journal of Colloid and Interface Science. 2011;363(1):348-54.
51. Mahdavinia GR, Rahmani Z, Karami S, Pourjavadi A. Magnetic/pH-sensitiveκ-carrageenan/sodium alginate hydrogel nanocomposite beads: preparation, swelling behavior, and drug delivery. Journal of Biomaterials Science, Polymer Edition. 2014;25(17):1891-906.
52. Tanzifi M, Tavakkoli Yaraki M, Beiramzadeh Z, Heidarpoor Saremi L, Najafifard M, Moradi H, et al. Carboxymethyl cellulose improved adsorption capacity of polypyrrole/CMC composite nanoparticles for removal of reactive dyes: Experimental optimization and DFT calculation. Chemosphere. 2020;255:127052.
53. Kannan N, Sundaram MM. Kinetics and mechanism of removal of methylene blue by adsorption on various carbons—a comparative study. Dyes and Pigments. 2001;51(1):25-40.
54. Tsai WT, Chang CY, Lin MC, Chien SF, Sun HF, Hsieh MF. Adsorption of acid dye onto activated carbons prepared from agricultural waste bagasse by ZnCl2 activation. Chemosphere. 2001;45(1):51-8.
55. Debrassi A, Corrêa AF, Baccarin T, Nedelko N, Ślawska-Waniewska A, Sobczak K, et al. Removal of cationic dyes from aqueous solutions using N-benzyl-O-carboxymethylchitosan magnetic nanoparticles. Chemical Engineering Journal. 2012;183:284-93.
56. Hamidzadeh S, Torabbeigi M, Shahtaheri SJ. Removal of crystal violet from water by magnetically modified activated carbon and nanomagnetic iron oxide. Journal of Environmental Health Science and Engineering. 2015;13(1).
57. Sharma G, Kumar A, Naushad M, García-Peñas A, Al-Muhtaseb AaH, Ghfar AA, et al. Fabrication and characterization of Gum arabic-cl-poly(acrylamide) nanohydrogel for effective adsorption of crystal violet dye. Carbohydrate Polymers. 2018;202:444-53.